Lateral periodicity and elastic stress relaxation in GaInAsP quantum wires on InP investigated by x-ray diffractometry

B. Jenichen[a] and H. T. Grahn
Paul-Drude-Institut für Festkörperelektronik, Hausvogteiplatz 5-7, D-10117 Berlin, Germany

T. Kojima and S. Arai
Research Center for Quantum Effect Electronics, Tokyo Institute of Technology, 2-12-1 O-okayama, Meguro-ku, Tokyo 152, Japan

(Received 3 December 1997; accepted for publication 6 March 1998)

Synchrotron x-ray diffractometry has been used to investigate GaInAsP quantum wire structures on InP with a quantum well layer between the substrate and the wire. The lateral periodicity was determined with high accuracy. An elastic stress relaxation, which occurs near the free surface of the sidewalls, was observed. It results in deformation gradients in the wires, which influence the distribution of the diffracted intensity in reciprocal space. © *1998 American Institute of Physics.* [S0021-8979(98)08311-X]

I. INTRODUCTION

The performance of semiconductor lasers is expected to greatly improve by introducing a quantum wire structure into the active region.[1–4] However, due to a low optical confinement and a poor size uniformity of multilayered quantum wire arrays, there have been some difficulties in reaching this goal. A new concept has been developed by adopting a relatively thick, compressively strained single quantum well as the basic material for the quantum wire structure.[5] An additional thin quantum well layer is introduced for partial support of the optical confinement and gain. This is of particular importance, when the wire width becomes very narrow and, as a consequence, the wavelength of the gain peak of the quantum wire almost coincides with that of the quantum-well layer. Using this approach, quantum wire lasers with low threshold and high differential quantum efficiency were obtained.[5] Their performance was compared with quantum well lasers fabricated on the same wafer. For these lasers a modified wet etching procedure was adopted.

Most of the previous x-ray investigations on surface gratings clarified the principles of the diffraction at gratings. However, these investigations were still concerned with lateral periodicities, which are much larger than the dimensions of the quantization.[6–10] Therefore, it was possible to apply triple crystal techniques for reciprocal space mapping[11,12] even with a sealed x-ray tube in order to obtain a considerable number of grating superstructure maxima. More recent work reached smaller periodicities of the wire gratings by utilizing high-intensity synchrotron sources.[13,14] In Ref. 13 the size dependent strain of $In_{0.2}Ga_{0.8}As/GaAs$ quantum wires was compared to photoluminescence data, while in Ref. 14 strain gradients in a buried $In_{0.2}Ga_{0.8}As/GaAs$ quantum wire array were observed.

In the present work, we have applied synchrotron x-ray diffractometry to investigate the lateral periodicity and elastic stress relaxation in InGaAsP quantum wire structures with a typical period of 70 nm, which were specially prepared for the x-ray investigations. The periodicity was determined with high accuracy from diffraction patterns for a symmetric (002) reflection. In order to distinguish strain relaxation effects due to the different InGaAsP layers in the wires from effects due to the patterning of the quantum wire array, we compare the diffraction patterns and reciprocal space maps in the vicinity of an asymmetric (113) reflection for a GaInAsP quantum wire system with those of a bare substrate with exactly the same grating pattern. An elastic relaxation of the InGaAsP wire structures near the free surface is observed.

II. EXPERIMENT

We investigated two patterned samples. Sample 1 is a reference sample with a grating structure on a bare p-InP substrate. A 20 nm thick SiO_2 layer was deposited by thermal chemical vapor deposition, and stripe masks were formed along the $\langle \bar{1}10 \rangle$ direction on the wafer by using electron beam lithography followed by reactive ion etching. Periodic SiO_2 stripe mask patterns were formed within areas of $0.4 \times 2.0\ mm^2$ with a separation larger than 1 mm. The actual wire structures were then fabricated by wet chemical etching using Br-methanol and H_2SO_4-based etchant. The epitaxial layer structure of sample 2 (schematically shown in Fig. 1) was prepared by low pressure organometallic vapor phase epitaxy (OMVPE) on a p-InP substrate. After a 2.0 μm thick p-InP buffer layer, and a 90 nm thick i-GaInAsP graded index (GRIN) optical confinement layer ($\lambda_g = 1.2-1.0\ \mu m$), the first compressively strained $Ga_{0.18}In_{0.82}As_{0.73}P_{0.27}$ single quantum well of 5 nm thickness ($\bar{\epsilon} = 1\%$) followed. A 12 nm thick i-$Ga_{0.22}In_{0.78}As_{0.47}P_{0.53}$ lattice matched barrier layer ($\lambda_g = 1.2\ \mu m$) separated the first well from the second, which is a compressively strained 10 nm thick $Ga_{0.18}In_{0.82}As_{0.73}P_{0.27}$ single quantum well ($\bar{\epsilon} = 1\%$). A second lattice matched barrier layer of i-$Ga_{0.22}In_{0.78}As_{0.47}P_{0.53}$ with a 5 nm thickness ($\lambda_g = 1.2\ \mu m$) followed. The whole structure was capped by a 5 nm thick i-InP layer. The lateral

[a]Electronic mail: jen@pdi-berlin.de

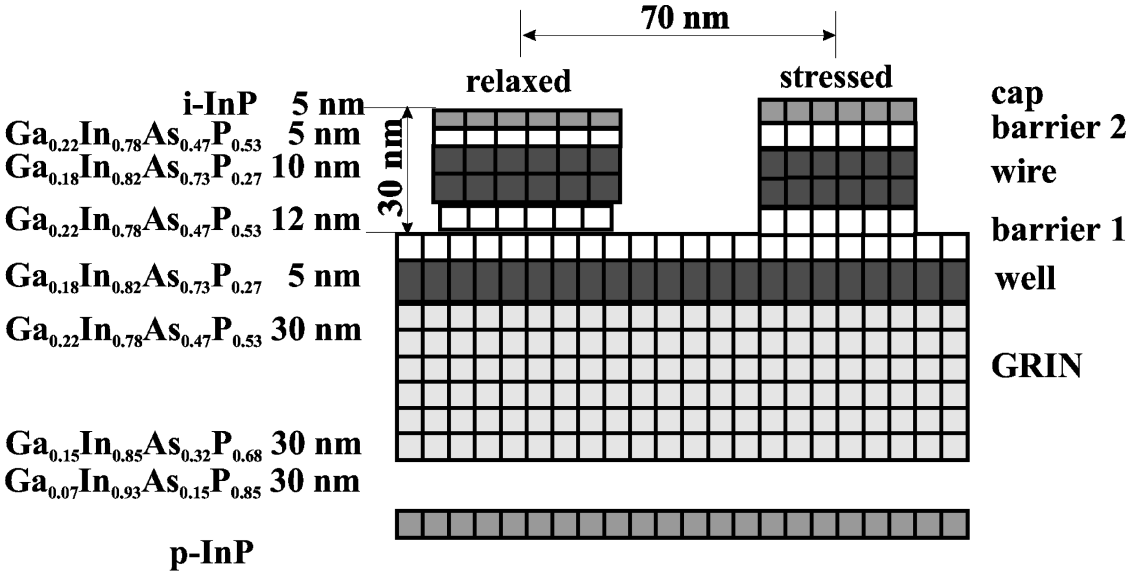

FIG. 1. Schematic diagram of the epitaxial layer system of sample 2, the dimensions of the wire structure, and possible stress states.

structure was obtained by the same procedure as for sample 1. The nominal etching depth was 25 nm for sample 1 and 30 nm for sample 2. A similar layer structure as sample 2 has been processed for laser structures. The respective optical properties are reported in Ref. 15. The comparison between the quantum-film and quantum-wire structure clearly confirmed two-dimensional size effects based on the anisotropy of the dipole moment in the quantum-wire structure.

The x-ray diffraction patterns were obtained with multiple crystal arrangements in the symmetrical geometry [InP (002) reflection] or in the extremely asymmetric InP (113) reflection[7] under grazing exit condition. For laboratory measurements Cu $K\alpha_1$ radiation from a 12 kW rotating anode source was monochromatized by two grooved Si (220) crystals.[16,17] Synchrotron radiation from the beam lines D4 [single crystal monochromator Ge (111), Ge (220) channel cut analyzer crystal] and W1 [double crystal monochromator Si (111), angular acceptance of the detector slits 3×10^{-3}] at HASYLAB was used for reciprocal space mapping. Figure 2 shows the geometrical relations in reciprocal space. **q** is the deviation of the scattering vector from the reciprocal lattice vector **H** of a given net plane ($\mathbf{q}=\mathbf{k}_e-\mathbf{k}_i-\mathbf{H}$). A scan of the sample alone (ω scan) is always directed perpendicular to the diffraction vector **H** (in particular in the symmetrical case, it is parallel to the surface, i.e., along the q_x direction). However, a scan of the detector by twice the angle of the sample rotation ($\omega/2\Theta$-scan) is directed parallel to the diffraction vector **H** (in the symmetrical case, it is perpendicular to the surface, i.e., along the q_z direction). A combination of these scans with different offsets yields a map of the reciprocal space near a certain Bragg reflection **H** (dots in Fig. 2). A surface grating leads to superstructure maxima in the vicinity of the Bragg peak lying on a line parallel to the surface (cf. Fig. 2). Due to the small periodicity of our quantum wire structures, these scans have to cover a relatively wide area of the reciprocal space. At the same time, the resolution can be kept relatively low, i.e., a slit collimation is sufficient for the asymmetric (113) reflection. In this case the large dimension of the slit aperture is directed perpendicular to the surface. The surface truncation leads to diffraction rods perpendicular to the surface,[18] which are modulated by the vertical structure of the sample (i.e., layer structure and etching depth).

III. RESULTS

The x-ray scattering from a quantum wire array can be described in the kinematical approximation in analogy to the Bragg diffraction from an atomic lattice.[19] Assuming that N grating periods of a length L are illuminated coherently by the x rays, the diffracted intensity around a Bragg reflection $\mathbf{H}=(h_x,h_y,h_z)$ is

$$I(\mathbf{q})=|f_p(\mathbf{q})|^2\left[\frac{\sin(Nq_xL/2)}{\sin(q_xL/2)}\right]^2, \tag{1}$$

$f_p(\mathbf{q})$ denotes the grating form factor of a single period, which modulates the intensities of the superstructure maxima

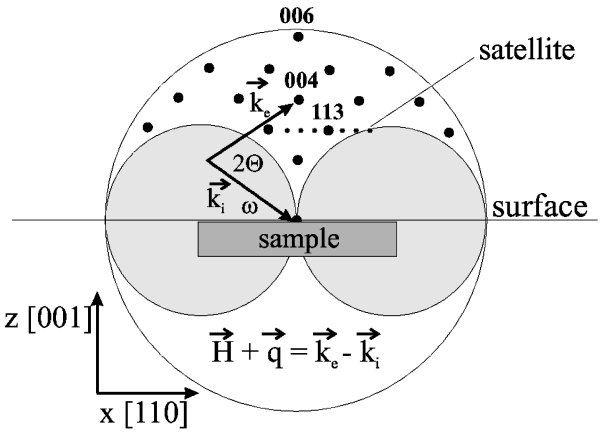

FIG. 2. Schematic diagram of the reciprocal space and the coordinate system in relation to the sample surface, which is oriented perpendicular to the z axis of our coordinate system. **q** is the deviation of the scattering vector from the reciprocal lattice vector **H** (symbolized by a large dot) of a given net plane ($\mathbf{q}=\mathbf{k}_e-\mathbf{k}_i-\mathbf{H}$).

like an envelope function, and **q** the momentum transfer measured from **H**. Introducing a deformation field inside the wires, e.g., in the direction parallel to the surface, results to first approximation in a shift of the grating form factor $f_p(\mathbf{q})$ by $h_x\epsilon_{xx}$,[20] where h_x is the component of the diffraction vector **H** along the surface in the direction perpendicular to the wire direction and ϵ_{xx} is the corresponding component of the average deformation tensor. Therefore, a strain in an otherwise coherent grating can be observed as a shift of the envelope function of the measured grating maxima. This envelope function is the Fourier transform of the shape function $s_p(\mathbf{r})$ of a single grating period.[6,20] The positions of the superstructure maxima remain unchanged, since coherency is preserved over the whole wire structure.[14]

The average lateral period of the surface grating was obtained from the angular distance of the first order superstructure peaks of the surface grating by performing a triple crystal ω scan along q_x near the symmetrical InP (002) reflection. The value for sample 1 is (70.3 ± 0.6) nm in good agreement with the anticipated periodicity. We could not resolve any broadening of the grating maxima compared with the resolution function of the triple crystal arrangement. Furthermore, no second order superstructure peaks were observed, because the widths of the grooves and the wires are equal.[8] The diffraction angle was determined very carefully, and the miscut of the InP substrate was verified to be negligible. The diffraction pattern for sample 1 near the InP (113) reflection measured with a laboratory source is shown in Fig. 3(a). The scattering intensities were recorded with a receiving slit with an angular acceptance of 2 mrad and correspond to an integration over q_z. The satellites exhibit a symmetrical distribution along q_x, i.e., the average deformation along the surface is zero ($\epsilon_{xx}=0$) as was confirmed by a fit of the envelope function $f_p(q_x+h_x\epsilon_{xx})$ to the experimentally obtained satellite maxima shown by the solid line in Fig. 3(a). From additional area scans, we know that along the q_z direction satellites of different order have the same shape. The satellites in the q_z direction do not show any splitting. Therefore, we assume for the individual wires as a first approximation a rectangular shape function convoluted with a Gaussian.[21] The half-width of the intensity maximum along q_z can be approximately correlated to the nominal etching depth.

The average lateral period of sample 2 was determined to be (69.4 ± 0.6) nm, which again corresponds to the nominal value. The ω scan near the InP (113) reflection for this sample shown in Fig. 3(b) exhibits a pronounced asymmetry of the envelope function of the satellite maxima along q_x. From the angular shift of this envelope function obtained by a fit of $f_p(q_x+h_x\epsilon_{xx})$ to the experimental satellite maxima as shown by the solid line in Fig. 3(b), the component of the average deformation along the surface in the patterned region is calculated to be $\epsilon_{xx}=(0.16\pm0.02)\%$. This deformation is due to the elastic relaxation of the internal stresses in the wires near the surface at the wire sidewalls.

The area map of the satellite pattern near the InP (113) reflection shown in Fig. 4 for sample 2 has been obtained with synchrotron radiation. The satellites of different order show interference fringes along the q_z direction. Only the top four epitaxial layers as shown in Fig. 1 undergo lateral structuring. For a q_z profile of the satellite reflection we have to take into account only those four layers. Preliminary calculations in the kinematical approximation show that the observed interference fringes along q_z correspond to those four layers in the wire ridges and, therefore, the anticipated etching depth. However, the various satellites show different shifts of the interference pattern along q_z indicating strain gradients in each of the wires.[14] These strain gradients were

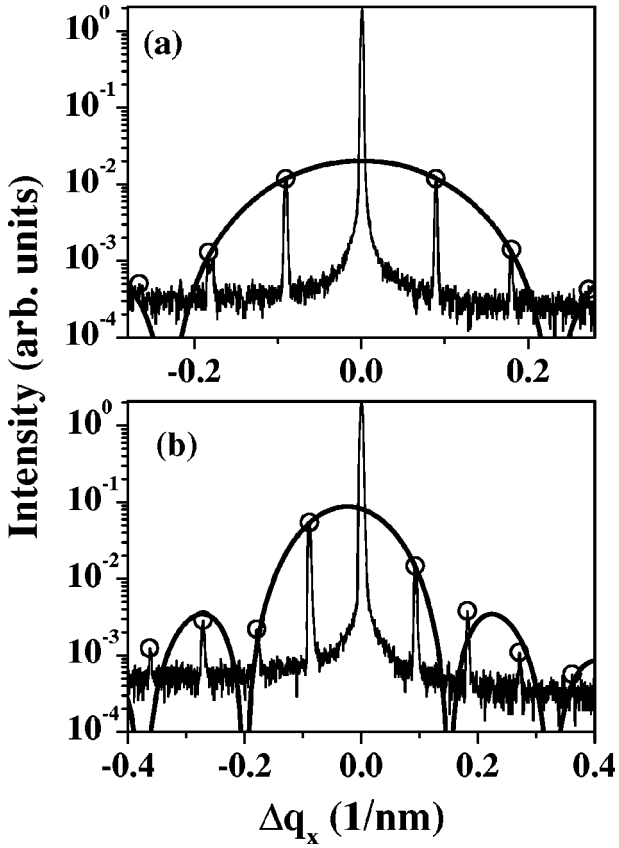

FIG. 3. ω scans near the InP (113) reflection intensity distribution integrated over q_z for the patterned InP substrate of sample 1 (a) and the InGaAsP quantum wire array of sample 2 (b) using Cu $K\alpha_1$ radiation of a rotating anode source. The solid lines are the shape functions $f_p(q_x+h_x\epsilon_{xx})$ fitted to the satellite maxima intensities.

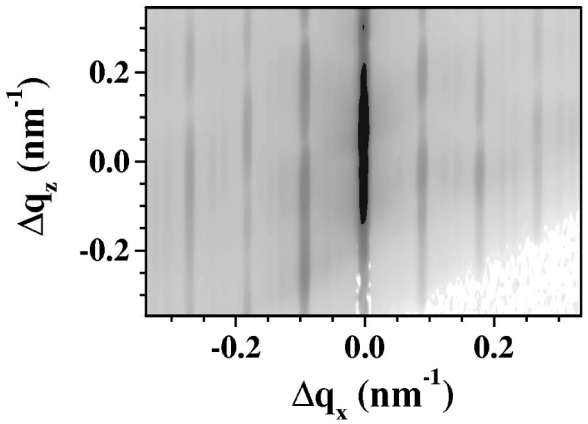

FIG. 4. Area map near the InP (113) reflection using synchrotron radiation ($\lambda=0.154$ nm) for sample 2.

not taken into account in our preliminary calculations. The zero-order satellite coincides with the surface truncation rod of the InP substrate. Near the substrate reflection, all eight epitaxial layers and the substrate contribute to the diffracted beam, including the material without any lateral structuring. This leads to a shape of the zero-order satellite different from the shape of all other satellites. The loss of intensity in the lower right corner of Fig. 4 is due to the fact that in this region the diffracted beam $\mathbf{k}_e$ does not have any component in the half-space above the sample.

Conventional $\omega/2\Theta$ scans along q_z were measured to study the unstructured part of sample 2 in order to characterize the unstructured layer structure independently. Although the Ga and As concentrations cannot be determined by x-ray measurements alone, a comparison with a dynamical simulation showed that the concentrations of the quaternary crystals are close to the nominal values. Therefore, in the following we will use the nominal concentrations. This implies that only the lattice parameters of the quantum well layer and the quantum wires differ by 1% from that of the substrate, while all other layers are nearly lattice matched to the substrate.

IV. DISCUSSION

The quantum well layer is tetragonally deformed. However, the deformation field in the quantum wires is expected to be more complicated.[22] For a first estimate, we will assume a fully relaxed wire structure (cf. Fig. 1) as in Ref. 23. These assumptions lead for the present wire orientation, $\langle \bar{1}10 \rangle$ on (001) InP, to a deformation of 1.55% perpendicular to the interface (similar to the tetragonal deformation of heteroepitaxial layers), while the deformation parallel to the interface, i.e., perpendicular to the wire orientation, is 1.01%. The lattice parameter along the wire direction $\langle \bar{1}10 \rangle$ is preserved over the whole layer system as in a continuous quantum well layer. This implies that a fully relaxed wire parallel to the $\langle \bar{1}10 \rangle$ direction would have an orthorhombic cell. However, the necessary condition for a fully relaxed wire is a height of the wire much larger than its width. This condition is obviously not fulfilled in our case, since we have a wire width of 35 nm, a wire height of 10 nm, and a vertical distance from the unpatterned material of about 10–15 nm. Since the etching depth amounts to 30 nm and the InGaAsP quantum wire height to 10 nm, only 1/3 of the grating ridges have a different lattice parameter. Furthermore, in Ref. 22 it was shown that for wires with a multiple quantum well structure the relaxation effects are concentrated near the edges of the wires. For example, in the $In_{0.2}Ga_{0.8}As/GaAs$ system, the elastic relaxation occurs mainly within the 4 nm thick surface region. Therefore, if the width of the quantum wire is much larger than 10 nm (as in our case), the elastic relaxation is mainly a surface phenomenon. For the wire width of our sample, the volume of the relaxed wire is reduced by another factor of more than 3. In total, the decreased volume of the relaxation region results in a reduction of the relaxation effect (i.e., of the average deformation along the surface) by approximately a factor of 10 compared with the model of the fully relaxed wire. This results in an expected deformation $\epsilon_{xx} \sim 0.1\%$, which agrees well with the elastic surface relaxation in sample 2 deduced from ω scan in Fig. 3(b). Therefore, no considerable deformations besides the elastic stress relaxation near the free surface are detected in our measurements. Of course, this elastic relaxation can be modified by a subsequent overgrowth of the grating pattern during the preparation of laser structures as reported in Ref. 13. Nevertheless, it should be taken into account in the interpretation of PL results obtained from free standing quantum wire arrays. The confinement of the carriers may be improved, and the carriers may be driven away from damaged surface regions by a modulation of the band structure due to surface relaxation in the wires.

V. CONCLUSIONS

The x-ray results confirm the average periodicity of the wire array with high accuracy. An elastic relaxation of the wires near the free surface of the sidewalls was observed. The surface relaxation leads to deformation gradients in the wires, which are probably responsible for the different positions of the interference maxima of the various satellites. In the future, this elastic relaxation will be correlated with the corresponding optical properties.

ACKNOWLEDGMENTS

The support of L. Lottermoser, O. Bunk, H. Rhan, M. Hanke, T. Wiebach, and M. Schmidbauer during the experimental work at HASYLAB is gratefully acknowledged. The authors thank T. Baumbach and V. Kaganer for helpful discussion.

[1] Y. Arakawa and H. Sakaki, Appl. Phys. Lett. **40**, 939 (1982).
[2] M. Asada, Y. Miyamoto, and Y. Suematsu, IEEE J. Quantum Electron. **QE-22**, 1915 (1986).
[3] Y. Arakawa and A. Yariv, IEEE J. Quantum Electron. **QE-22**, 1887 (1986).
[4] Y. Miyake and M. Asada, Jpn. J. Appl. Phys., Part 1 **28**, 1280 (1989).
[5] T. Kojima, M. Tamura, K.-C. Sin, S. Tamura, and S. Arai, in *Digest of Eighth International Conference on Indium Phosphide and Related Materials* (IEEE, New York, 1996), pp. 731–734.
[6] Q. Shen, C. C. Umbach, B. Weselak, and J. M. Blakely, Phys. Rev. B **48**, 17967 (1993).
[7] A. T. Macrander and S. E. G. Slusky, Appl. Phys. Lett. **56**, 443 (1990).
[8] L. Tapfer and P. Grambow, Appl. Phys. A **50**, 3 (1990).
[9] A. A. Darhuber, E. Koppensteiner, H. Straub, G. Brunthaler, W. Faschinger, and G. Bauer, J. Appl. Phys. **76**, 7816 (1994).
[10] G. T. Baumbach and M. Gailhanou, J. Phys. D **28**, 2321 (1995).
[11] A. Iida and K. Kohra, Phys. Status Solidi A **51**, 533 (1979).
[12] P. F. Fewster, Crit. Rev. Solid State Mater. Sci. **22**, 69 (1997).
[13] Q. Shen, S. Kycia, E. S. Tentarelli, W. J. Schaff, and L. F. Eastman, Phys. Rev. B **54**, 16381 (1996).
[14] Q. Shen and S. Kycia, Phys. Rev. B **55**, 15791 (1997).
[15] T. Kojima, M. Tamura, X.-Y. Jia, H. Nakaya, T. Ando, S. Tanaka, S. Tamura, S. Arai, and G. Bacher, Jpn. J. Appl. Phys. **37**, (1998).
[16] W. M. Du Mond, Phys. Rev. **52**, 872 (1937).
[17] N. Loxley, B. K. Tanner, and D. K. Bowen, J. Appl. Crystallogr. **28**, 314 (1995).
[18] I. K. Robinson and D. J. Tweet, Rep. Prog. Phys. **55**, 599 (1992).
[19] B. E. Warren, *X-Ray Diffraction* (Addison-Wesley, New York, 1969).
[20] V. Holy, A. A. Darhuber, G. Bauer, P. D. Wang, Y. P. Song, C. M. Sotomayor Torres, and M. C. Holland, Phys. Rev. B **52**, 8348 (1995).
[21] M. Tamura, Y. Nagashima, K. Kudo, K.-C. Shin, S. Tamura, A. Ubukata, and S. Arai, Jpn. J. Appl. Phys., Part 1 **34**, 3307 (1995).
[22] L. De Caro, L. Tapfer, and A. Giuffrida, Phys. Rev. B **54**, 10575 (1996).
[23] L. De Caro and L. Tapfer, Phys. Rev. B **49**, 11127 (1994).